Journal of Geomatics Vol 12 No. 1 April 2018

A comparative analysis of the performance of GNSS permanent receivers at the Centre for Geodesy and Geodynamics, Nigeria

Olalekan Adekunle Isioye[1], Mefe Moses[1], Farouk Musa Isa[1] and Mohammed Bojude[2],
[1]Department of Geomatics, Ahmadu Bello University, Zaria-Kaduna State, Nigeria
[2]Centre for Geodesy and Geodynamics, National Space Research Agency, Toro- Bauchi state, Nigeria
Email: lekkyside4u@yahoo.com, oaisioye@abu.edu.ng

(Received: Feb 14, 2018; in final form: Apr 13, 2018)

Abstract: This study compares the performance of two continuously operating Global Navigation Satellite System (GNSS) receivers at the Toro observatory in Nigeria. The observatory is a proposed site for part of the global geodetic core network for collocation of GNSS and other space geodetic techniques. The pair of GNSS receivers (Ashtech UZ-12 and Trimble NetR8) are connected via a GNSS splitter to a single antenna (Trimble GNSS Choke Ring TRM59800.00). Observation files, precise orbit and clock files, and satellite differential code bias files with respect to the two receivers were collected for a period of 30 days. The WaSoft software (WaPPP module) was employed to estimate the receivers' position, zenith tropospheric delay (ZTD) and tropospheric gradients. Also, the Gopi software was used to estimate the receivers' bias and total electron content (TEC). The resulting parameters from the estimation software were subjected to hypothetical testing using the Student t-test based on the Bland Altman method of analysis for comparison tests. The results of the statistical tests show that the choice of GNSS receiver does affect the estimation of Z-component of the coordinate, ZTD, receiver bias and TEC at 95% confidence level. However, the results show that the X and Y-components of the receivers' position and tropospheric gradients were not influenced by the choice receiver. The results obtained from this study pinpoint the need to ascertain the accuracy of parameters estimated from geodetic grade receivers and ensure that the parameters do not differ significantly from each other, particularly when these are required for very precise scientific applications.

Keywords: Global Navigation Satellite System (GNSS), receiver bias, tropospheric gradients, total electron content (TEC), zenith tropospheric delay (ZTD), performance and analysis of receivers

1.0 Introduction

Global Navigation Satellite System (GNSS) ground infrastructure is on the increase globally; the ground infrastructure comprises many hundreds (if not thousands) of continuously operating reference stations (CORSs). As the name suggests, this GNSS infrastructure typically comprises GNSS receivers, antennas and computer systems (identical to surveying user equipment). The highest CORS tier is the network of stations that contributes to the international GNSS service (IGS), and in effect makes up part of the physical infrastructure of the global geodetic observing system. Such CORS stations have well-established, very stable monuments, and operate continuously for many years. The IGS supports the realisation of the international terrestrial reference frame and the determination of highly accurate satellite orbit and clock products to facilitate techniques such as precise point positioning (PPP) (Kouba, 2009).

GNSS-CORS data consist of carrier phase and code range measurements in support of three-dimensional positioning, agriculture, construction, meteorology, space weather, seismology and other geophysical applications across the globe (Rizos, 2007; Dow et al., 2009). GNSS-CORS are typically operated by scientific agencies, government departments (federal, state and local), private companies and academia, but even individuals. Furthermore, these CORS have the task to store data, in some circumstances process the data, and then transmit these data to roving receivers. These CORS help users by economising on one GNSS receiver, as the operation of the reference station is performed by the service provider of the CORS network.

Every CORS network consists of several GNSS stations interconnected by reliable communications to enable real-time computations and control. Each station has a minimum requirement of a receiver, an antenna, communications and a power supply. In most cases, a computer is installed additionally for data transmission and control. The precision of results differs for the different users or applications of CORS. The precision of results for the different applications also depends on the type of ground infrastructure (receiver, antenna, and cabling options) and computer accessories, which include software.

The CORS antenna tracks signals emitted by a satellite in space and these signals follow a path from the satellite mounted in space, propagating through the atmosphere and down to the receiver located on the surface of the earth. In the process of transmission, the signal undergoes a lot of delay along its path, which reduces its strength, and in some cases diverts or breaks the signal path, causing error in signal transmission. However, satellite signal propagation and antenna error can be mitigated with appropriate correction schemes

(Chuang and Gupta, 2013). More so, several studies have evolved to develop and validate multi-antenna GNSS receiver systems that can perform excellently even under jamming attacks or resilient navigation (Vagle et al., 2016; Gupta et al., 2016; Cuntz et al., 2016).

The influence of the choice of permanent GNSS receivers, receiver architecture, settings and stability of estimated parameters from satellite signals for the different users and applications have received attention from different researchers. Zhang et al. (2010) performed a series of tests using highly sensitive (HS) receivers and a number of geodetic and navigation grade antennas in order to examine the variation in their performance. The study reveals clear advantages of using HS receivers instead of conventional receivers in applications requiring meter level accuracies with moderate antenna dynamics.

Odolinski and Teunissen (2016) compared the performance of a low-cost ublox single-frequency dual system (SF-DS) to that of a dual-frequency single system (DF-SS), based on much more expensive survey-grade receivers. The experiment revealed that SF-DS has the potential to achieve comparable ambiguity resolution performance to that of a DF-SS (L1, L2 GPS), based on the survey-grade receivers. High-sensitivity low-cost receivers have thousands of correlators to reduce the search space of each correlator and are able to acquire signals with low decibel watt (Schwieger, 2007).

The performance of low-cost single-frequency receivers can be improved by using a geodetic grade antenna instead of the low-cost single-frequency antenna (Takasu and Yasuda, 2008). In addition, Sousa and Nunes (2014) studied the influence of receiver architecture on the estimated parameter (ionospheric scintillation, multipath and high dynamics motion) from satellite signals. The study analysed the gains and drawbacks of a vector delay/frequency-locked loop architecture regarding the conventional scalar and the vector delay-locked loop architectures for GNSS receivers in harsh scenarios that include ionospheric scintillation, multipath and high dynamics motion.

From the foregoing, it is evident that since low-cost single-frequency receivers became available, several attempts have been made to reduce the cost and increase the accuracy of such receivers compared with geodetic grade receivers. Very little attention is paid to the accuracy of estimated parameters from geodetic grade GNSS receivers themselves. Many permanent GNSS installations have unique cabling requirements. Depending on the available infrastructure, the antenna may need to be mounted at a substantial distance from the receiver. The degree of loss in a coaxial cable depends on the frequency of the signal passing through it. There are no universal conventions in terms of the type of receivers or cabling options for varying applications. Thus it is imperative to ascertain if the choice of GNSS receiver does affect the parameters estimated for the satellite signals.

In this study, we compared the accuracies of the two geodetic receivers at the Centre for Geodesy and Geodynamics (CGG) in Toro, Nigeria. The two receivers operated by different agencies (Jet Propulsion Laboratory (JPL) and the office of the Surveyor General of the Federation (OSGOF, the Nigerian mapping agency)) both receive signals from the same antenna (single antenna) via a connection from a GNSS splitter. The result of the present study would be a great contribution to user knowledge in relation to GNSS-CORS in Nigeria and the world at large. The strategic relevance of CGG Toro as the only geodetic observatory in Nigeria and the host of the only IGS station in Nigeria further highlights the significance of the study. The datasets, hypothesis and analysis method used in this study are described in section 2. Results and discussions on the estimated parameter from the two receivers is presented in Section 3. Concluding remarks are presented in the final section.

2.0 Materials and methods

The scope of this research work covers comparative analysis of the positional accuracy, receiver biases, ionosphere and tropospheric parameter estimates in Toro observatory of the National Space Research Agency from permanent geodetic grade GNSS receivers, both connected to a single geodetic grade antenna via a GNSS splitter.

The stages of this study involve four tasks with reference to the schematic diagram, figure 1. The first is to acquire experimental data, the second to process the data for the experiment, the third to compare the results obtained from the processing and the last to analyse and draw conclusions, as well as present the data.

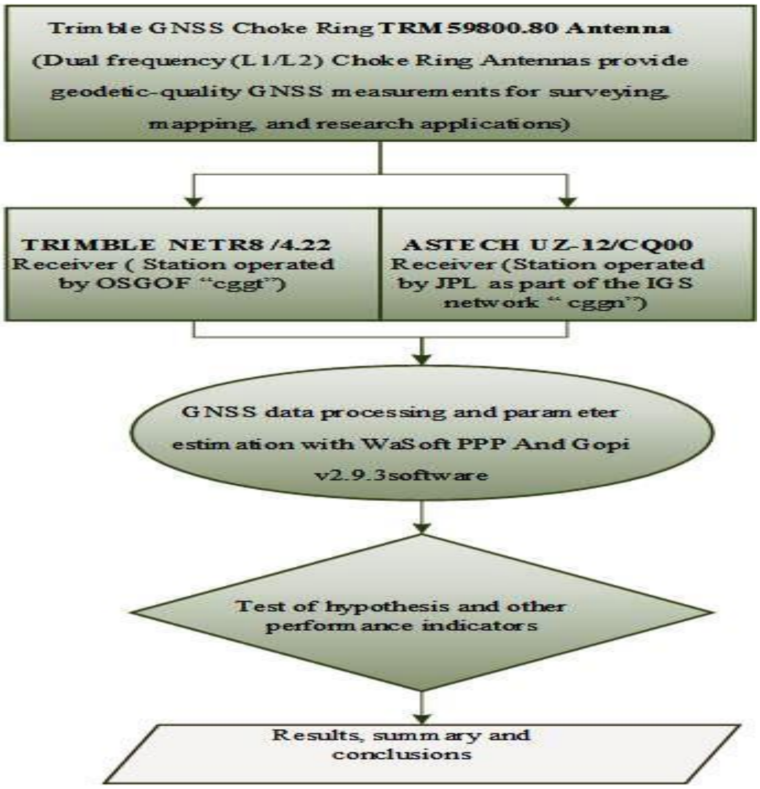

Figure 1: Schematic diagram of methodology

2.1 GNSS station location and instrumentation

The CGG located at Toro LGA in Bauchi State in North Central Nigeria is one of the seven centres of NASRDA. The Toro Observatory is situated on a part of the Basement Complex of Nigeria. It is composed of older granites and magmatites. These geological features that occur in these areas necessitated the choice of the Geodetic and Geodynamics Observatory site. In addition, the site has surface expressions of the West African Craton – an ancient, stable core of the African continent that has not been deformed over geological time. This large igneous unit is representative of the most stable region of Africa (corresponding to the Canadian Shield in North America). The CGG is central to geodetic activities in Nigeria; the observatory is the host to the only IGS station in Nigeria (Figure 2). OSGOF also has one of its numerous GNSS stations across the country located in the observatory of CGG. The centre streams GNSS raw data from CGGN to the JPL. The CGGN is archived at the Crustal Dynamics Data Information Centre (CDDIS). Similarly, GNSS data from CGGT are streamed to OSGOF's office located in Abuja, the federal capital city. The OSGOF receiver (CGGT) is the Trimble NET R8 receiver version 4.22 and the receiver for CGGN is an ASTECH UZ-12 receiver version CQ00 (Figure 3). The NetR8 GNSS reference receiver is a multiple-frequency GNSS receiver. It can track all GPS signals (L1/L2/L5) as well as GLONASS (L1/L2). The Trimble NetR8 receiver is designed to serve in all common geodetic reference receiver roles. This receiver also has specialised capabilities that make it an excellent reference receiver for scientific applications. The NetR8 receiver provides a TNC-type female connector for connecting to an antenna. The receiver is intended for use with a Zephyr™ Geodetic Model 2 antenna or a Trimble GNSS Choke Ring antenna. The Ashtech UZ-12 processes signals from the GPS satellite constellation, deriving real-time position, velocity and time measurements. The Ashtech UZ-12 receives satellite signals via an L-band antenna and low-noise amplifier (LNA). The receiver operates as a stand-alone reference station providing raw measurements, and as a real-time differential base station broadcasting (DGPS) corrections based on code-phase, and real-time kinematic mode. The receiver features 12-parallel channel/12-space vehicle (SV) all-in-view operation; each of up to 12 visible SVs can be assigned to a channel and then continuously tracked. Each SV broadcasts almanac and ephemeris information every 30 seconds, and the unit automatically records this information in its non-volatile memory. The unit has an L1/L2-band radio frequency port and four RS-232 serial input/output ports. Ports A, B, C, and D are capable of two-way communication with external equipment. Ports A and B have expanded support for more advanced communication strategies. The receiver permits uninterrupted use even when anti-spoofing (AS) is turned on. When AS is on, the receiver automatically activates our patented Z-tracking mode that mitigates the effects of AS. A GNSS splitter connects the two receivers (CGGT and CGGN) to a Trimble choke ring TRM59800.80 antenna (Figure 3).

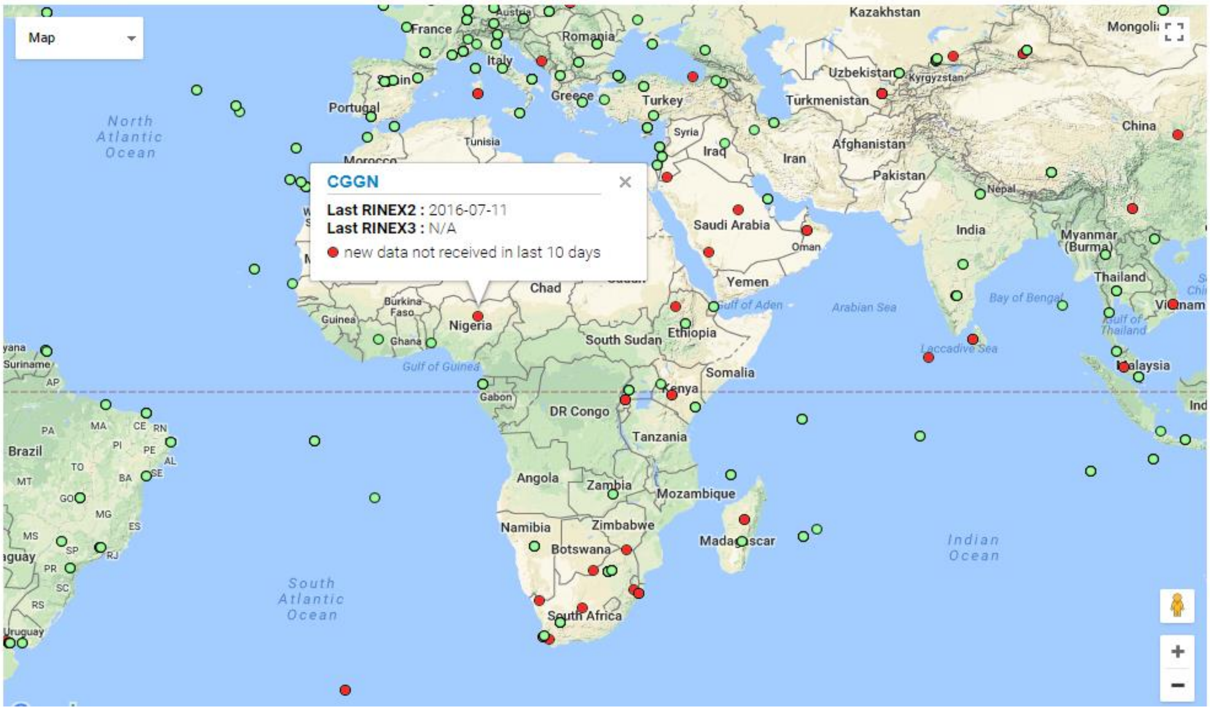

Figure 2: IGS network showing location of IGS station (CGGN) in Nigeria (after www.igs.org)

Figure 3: GNSS CORS antenna and receivers in Toro: A) Antenna (TRM59800.00), B) CGGT Trimble NET R8 Receiver, C) CGGN Ashtech UZ-12

Trimble GNSS Choke Ring TRM59800.00 (Dual frequency (L1/L2) Choke Ring) antennas provide geodetic-quality GNSS measurements for surveying, mapping, and research applications. Typical dual-frequency choke ring antennas maintain a stable phase centre that has less than 1 mm of drift. The choke ring antenna is based on the geodetic research standard and features aluminium choke rings and a Dorne Margolin antenna element. This antenna is very durable and has low power consumption and excellent multipath rejection characteristics. The Trimble GNSS Choke Ring TRM59800.00 is a TRM29659.00 reworked with a wide-band LNA for GNSS.

2.2 GNSS Data Download and Processing

Observation and navigation data for CGGT were obtained from the Nigerian GNSS Network (NIGNET) download site. The NIGNET comprises 14 other stations aside from the CGGT; it is the primary network for the new Nigerian geocentric datum (Jatau et al., 2010; Dodo et al., 2011; Naibbi and Ibrahim, 2014). The capability of the NIGNET in varying scientific applications (i.e., meteorological and space weather studies) has been demonstrated (Isioye et al., 2017a & b; Moses et al., 2017). Similarly, observation and navigation data for the CGGN were downloaded from the Scripps Orbit and Permanent Array Center (SOPAC) website via the CDDIS website; both sets of data were obtained in RINEX2.X format.

In additional, broadcast ephemerides for GLONASS channel numbers in RINEX format, a satellite and antenna phase correction file in ANTEX format, precise satellite orbit files in SP3 format, precise clock correction files in RINEX-CLK format, and satellite differential code bias (DCB) files were obtained. Table 1 is a summary of the different data types and their download sources. Thirty-day data were downloaded for the month of January 2012; the days were common to both stations and the network (CGGT and CGGN). The RINEX data were compressed files and so the files were unzipped using the Win-rar unzipper. The files were extracted and converted from D files to O files (observation files) by using the CRX2RNX and unpack applications. To achieve the objective of this study, we employed Wasoft software and GPS-TEC analysis v2.2 software in processing of all downloaded GNSS data and products.

The Wasoft software is modular GNSS processing software with the capability of PPP processing for GNSS observation of single stations. The PPP engine or "WaPPP" is capable of automatic processing without user interaction and suitable for batch processing. WaPPP computes coordinates based on GNSS observations in RINEX format; it also provides the option for the estimation of tropospheric delay and tropospheric gradients. It is useful for obtaining sub-metre, decimetre, or centimetre level accuracies. The highest accuracies require long-term (a few to many hours) of continuous dual-frequency carrier-phase observations in addition to precise satellite orbits and clock corrections, satellite antennas and user antenna corrections. WaPPP weights the different observations types (code and carrier phase, various GNSS) according to a variance component estimation. It uses a robust estimation algorithm in the estimation of position results and other estimated parameters.

Table 1: Station data and sources

Sr. No.	Data description	Data Source
1	Daily observation and navigation data in compacted RINEX format from the NIGNET for 'CGGT'	www. nignet.net
2	Daily observation and navigation data in compacted RINEX format from the NIGNET for 'CGGN'	ftp//cddis.gsfc.nasa.gov/pub/~gps/products
3	Ephemerides data GLONASS(.g file)	ftp//cddis.gsfc.nasa.gov/pub/~glonass/products/
4	Precise satellite correction data from IGS (.sp3 file)	ftp//cddis.gsfc.nasa.gov/pub/~gps/products
5	Final IGS clock product (.clk file)	ftp//cddis.gsfc.nasa.gov/pub/~gps/products
6	Antenna correction file from IGS (igs08.atx)	ftp//cddis.gsfc.nasa.gov/pub/~station/general/igs08.atx
7	Satellite differential code bias	(ftp://ftp.unibe.ch/~aiub/CODE

The WaPPP engine processes GNSS data for the CGGN and CGGT with the option of outputting the 3D station coordinates, zenith tropospheric delay and tropospheric gradient components. The GPS-TEC analysis v2.2 software (http://seemala.blogspot.com) is free software for the estimation of total electron content (TEC) from GPS observations developed by Gopi Seemata at Boston College, USA. The features of this software application include the ability to batch process the input files (RINEX and others). It also has the ability to download the navigation file automatically were necessary. Using the available GNSS data, satellite navigation data and the DCB files, the TEC was processed from the GPS-TEC analysis software for the two receivers. In addition, the software estimates DCBs (along with the inter-channel biases for different satellites in the receiver) for the ground GNSS station.

2.3 Statistical analysis and hypothesis testing

Based on comprehensive evaluation of the different parameters (station coordinates, ZTD, tropospheric gradients, TEC, and receiver bias) estimated from the two receivers, we use the Bland Altman method validation/method comparison test. The Bland Altman analysis in XLSTAT software estimates bias, using the chosen criterion (difference, difference in percentage, or ratio), the standard error, Pearson correlation coefficient, and difference and Bland Altman plots. The bias is the mean of the differences between the two methods, in this case Trimble NET R8 receiver version 4.22 (CGGT) and ASTECH UZ-12 receiver version CQ00 (CGGN). The standard error is computed, as well as a confidence interval. Ideally, the confidence interval should contain zero. The Bland Altman plot displays the difference between the two methods (receivers) for visualisation. XLSTAT software displays the correlation between the abscissa and the ordinates. One would expect it to be non-significantly different from zero, which means the confidence interval around the correlation should include zero. Next, one has the results of the Student t-test, performed on the means for each receiver. This test computes the difference between the two for each receiver, and checks whether it is different from zero or not. This test requires the assumption that the differences are normally distributed. Thus, the t-test helps to test the hypothesis on the influence of the choice of GNSS receiver on the estimated parameters from GNSS satellite signals. The null hypothesis (H_0) and alternative hypothesis (H_1) are as follows:

i. Null hypothesis H_0 states that mean ($\mu1-\mu2=0$): the choice of GNSS receivers does not affect the estimated parameters from GNSS satellites in the study area.

ii. Alternative hypothesis H_1 states that mean ($\mu1-\mu2\neq0$): the choice of GNSS receiver affects the estimated parameters from GNSS satellites in the study area.

3.0 Results and discussion

This section presents the results of the various tests for the performance comparison for the two receivers. The discussions cover the different parameters estimated from the receivers, which include the 3D position estimates, tropospheric parameters (ZTD and tropospheric gradients), TEC and receiver differential biases.

3.1 3D position information

The computed geographic coordinates from the Wasoft software were converted to the Universal Traverse Mercator (UTM) system for easy comparison. The daily series plot of the 3D coordinate values is shown in figure 4.

Table 2: Summary of the descriptive statistics for information on the receivers' position

Stn	Min	Max	Mean	Std Dev
Easting (X-component)				
CGGT	512961.537	512961.552	512961.548	0.003
CGGN	512961.546	512961.552	512961.549	0.002
Northing (Y-component)				
CGGT	1119024.705	1119024.709	1119024.707	0.001
CGGN	1119024.704	1119024.709	1119024.706	0.001
Height (Z-component)				
CGGT	916.443	916.454	916.448	0.003
CGGN	916.442	916.453	916.447	0.003

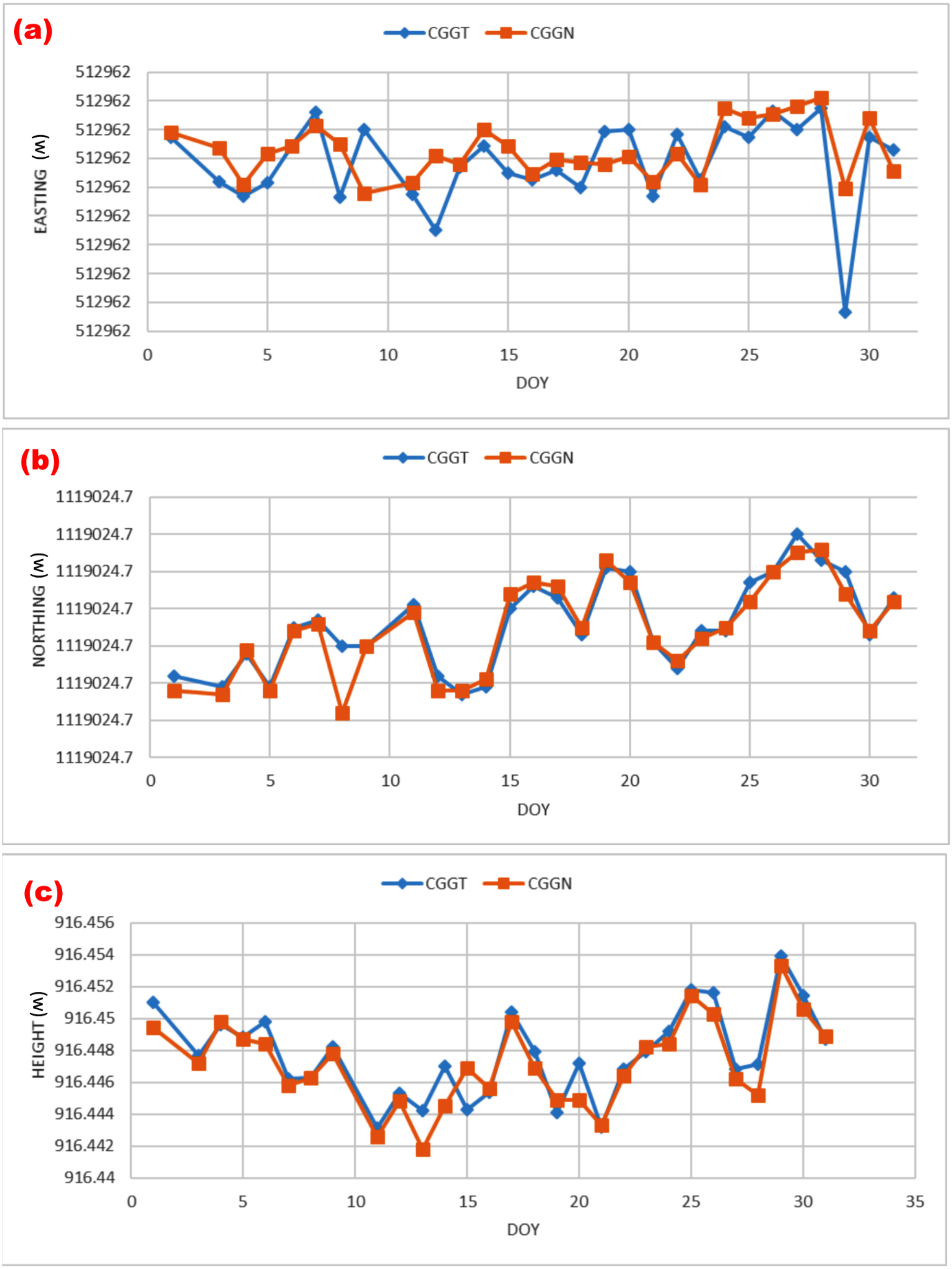

Figure 4: Time series plot of estimated coordinates from the two receivers: a) is the northing or y-component in metres b) is the easting or x-component in metres and c) is the height or z-component in metres

The summary of the statistics of the estimated position of the two receivers is presented in Table 2. The positional estimates do not show much variation. The Pearson correlation coefficient from scatter plots comparing CGGT and CGGN (Figure 5) reveals a strong relation of 0.604, 0.944, and 0.928 for the X, Y, and Z components of the position for the receivers, respectively.

The Bland and Altman estimate of bias is 8.28E-04, -1.103E-04, and -5.724E-04, for the X, Y, and Z component, respectively. The difference (Bland and Altman) plot displays the difference between the estimated coordinates from CGGN and CGGT against their average value, as shown in Figure 6. There was good agreement between the two receivers, since most of the data fall within the 95% confidence interval of the bias and standard error. The estimated p-value from the Student t-test is 0.070, 0.165, and 0.006, for the X, Y, and Z components, respectively. Thus, the computed p-value is greater than the significance level alpha = 0.05 for the X and Y components. The null hypothesis H_0 cannot be rejected for the X and Y component and the risk of rejecting the null hypothesis H_0 is 6.98% and 16.51%, respectively. Conversely, the t-test results for the height component show that the computed p-value is lower than the significance level alpha = 0.05. The null hypothesis H_0 was rejected; the risk of rejecting the null hypothesis H_0 while it is true is lower than 0.59%.

3.2 Tropospheric parameters

The descriptive statistics for the estimated tropospheric parameters (ZTD, tropospheric gradient E-N components) from CGGN and CGGT receivers are contained in Table 3. The Pearson correlation coefficient from the scatter plot comparing ZTD at CGGT and CGGN (Figure 7) reveals a very strong relation of 0.970. A time series plot of the different tropospheric parameters is presented in Figure 8.

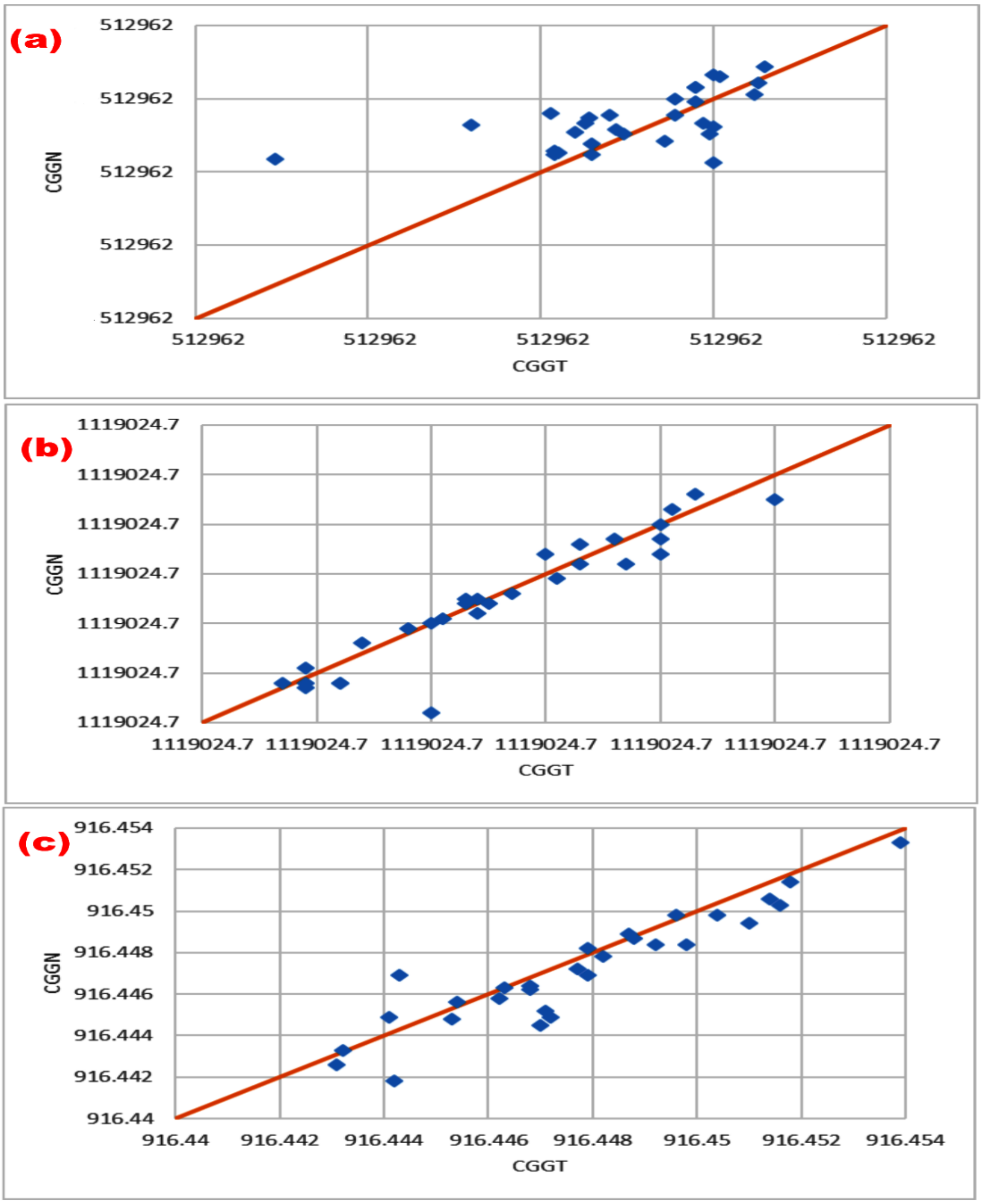

Figure 5: Scatter plots of estimated coordinates from the two receivers: a) is the northing or y-component b) is the easting or x-component and c) is the height or z-component

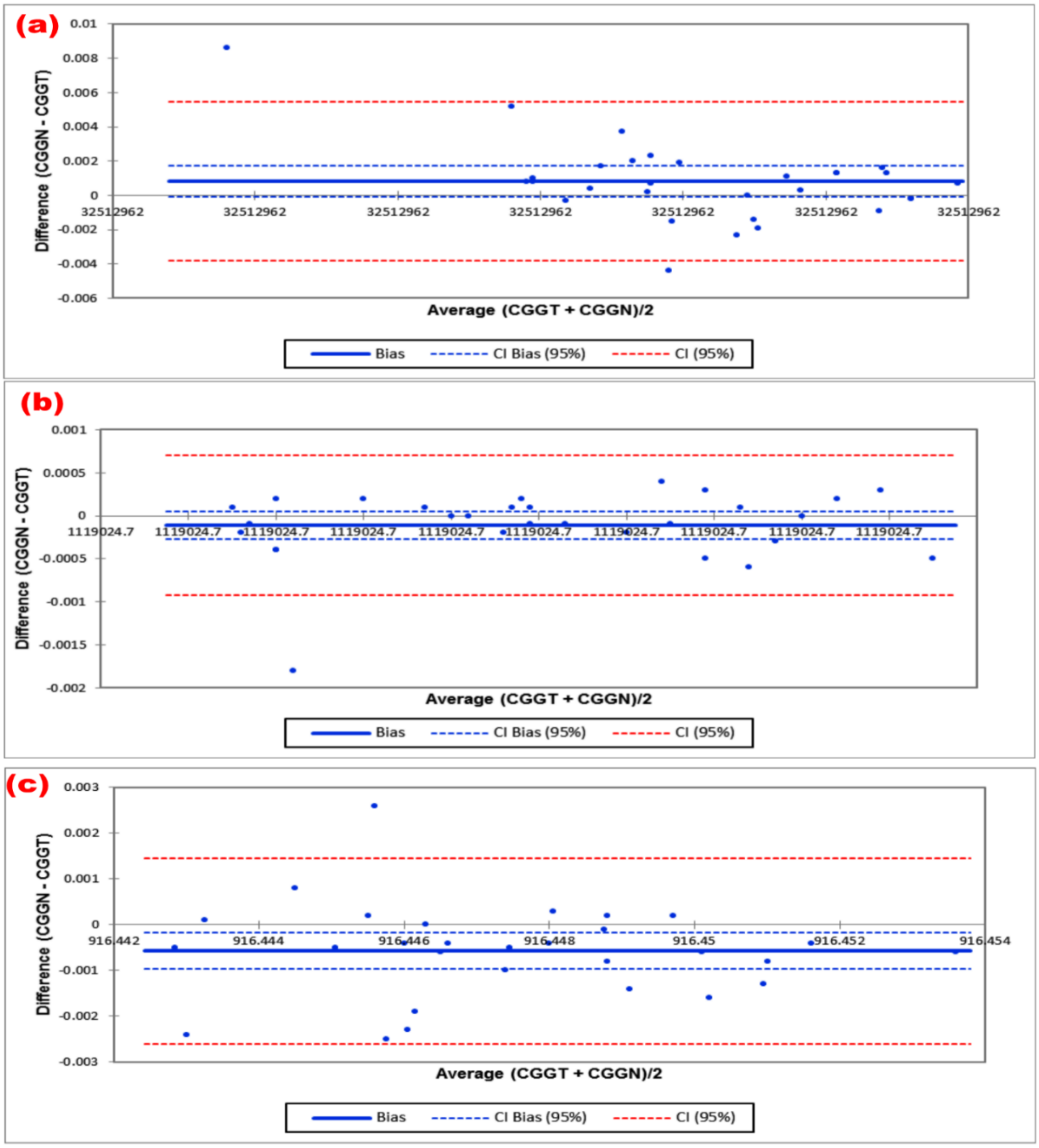

Figure 6: Bland and Altman (difference) plot of estimated coordinates from the two receivers: a) is the northing or y-component in metres b) is the easting or x-component in metres and c) is the height or z-component in metres

Table 3: Summary of the descriptive statistics for estimated tropospheric parameters

Station	Min	Max	Mean	Std Dev
ZTD (m)				
CGGT	2.125	2.181	1.151	0.011
CGGN	2.122	2.186	1.150	0.011
Tropospheric Gradient (E-component (m))				
CGGT	-0.006	0.002	-0.002	0.002
CGGN	-0.006	0.003	-0.002	0.002
Tropospheric Gradient (N-component (m))				
CGGT	-0.004	0.000	-0.002	0.001
CGGN	-0.005	0.000	-0.002	0.001

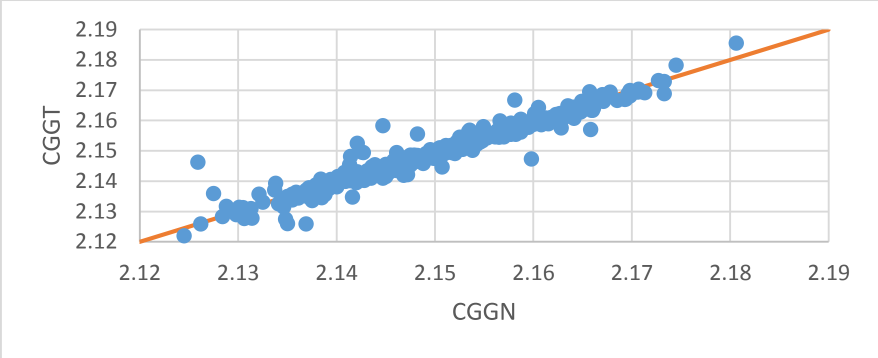

Figure 7: Scatter plot of estimated ZTD from the two receivers

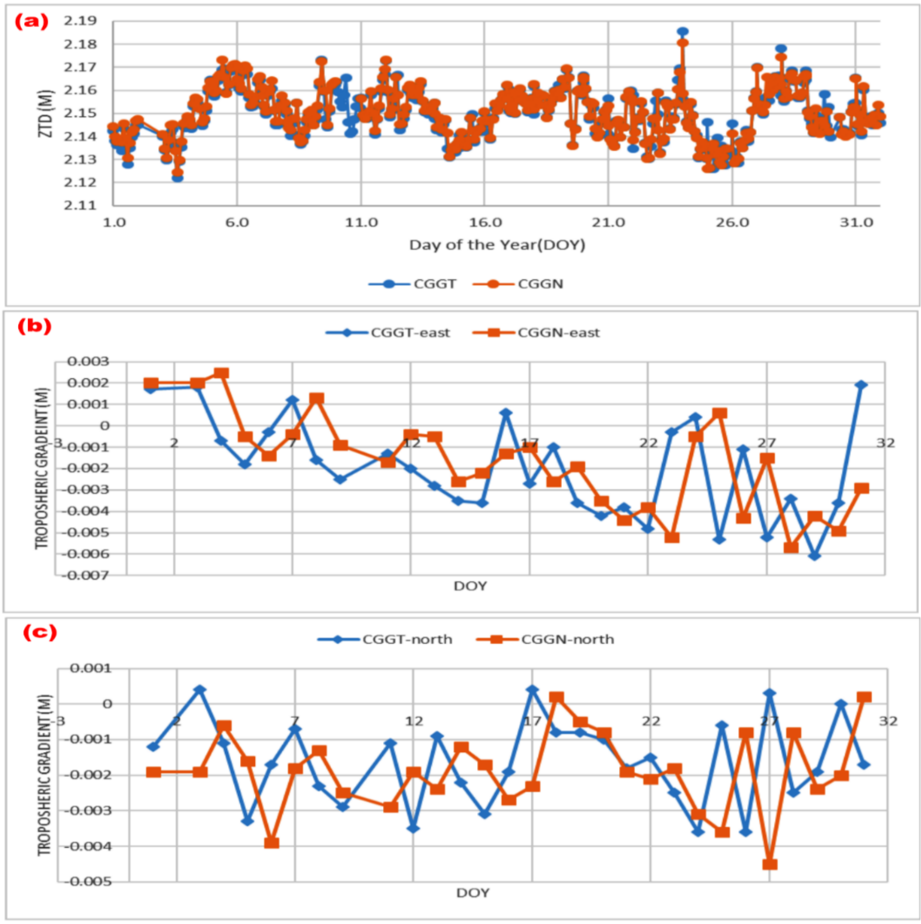

Figure 8: Time series plot of estimated tropospheric parameters from the two receivers; a) is the ZTD in metres b) is the tropospheric gradient (east component) in metres and c) is the tropospheric gradient (north component) in metres

The Bland and Altman estimate of bias is 4.876E-04, 2.655E-04, and -5.552E-04, for the ZTD, east component, and the north component of the tropospheric gradients, respectively. The difference (Bland and Altman) plot displays the difference between the estimated coordinates from CGGN and CGGT against their average value as shown in figure 9. There are was good agreement in ZTD estimates between the two receivers, since most of the data fall within the 95% confidence interval of the bias. The estimated p-value from the Student t-test is 0.000, 0.562, and 0.440, for the ZTD, east component, and the north component of the tropospheric gradients, respectively. Thus, the computed p-value is greater than the significance level alpha = 0.05 for the east component, and the north component of the tropospheric gradients. The null hypothesis H_0 cannot be rejected for the east component, and the north component of the tropospheric gradients and the risk of rejecting the null hypothesis H_0 is 56.24% and 43.97%, respectively. Conversely, the t-test results for the ZTD show that the computed p-value is lower than the significance level alpha = 0.05, and the null hypothesis H_0 is rejected; the risk of rejecting the null hypothesis H_0 while it is true is lower than 0.03%.

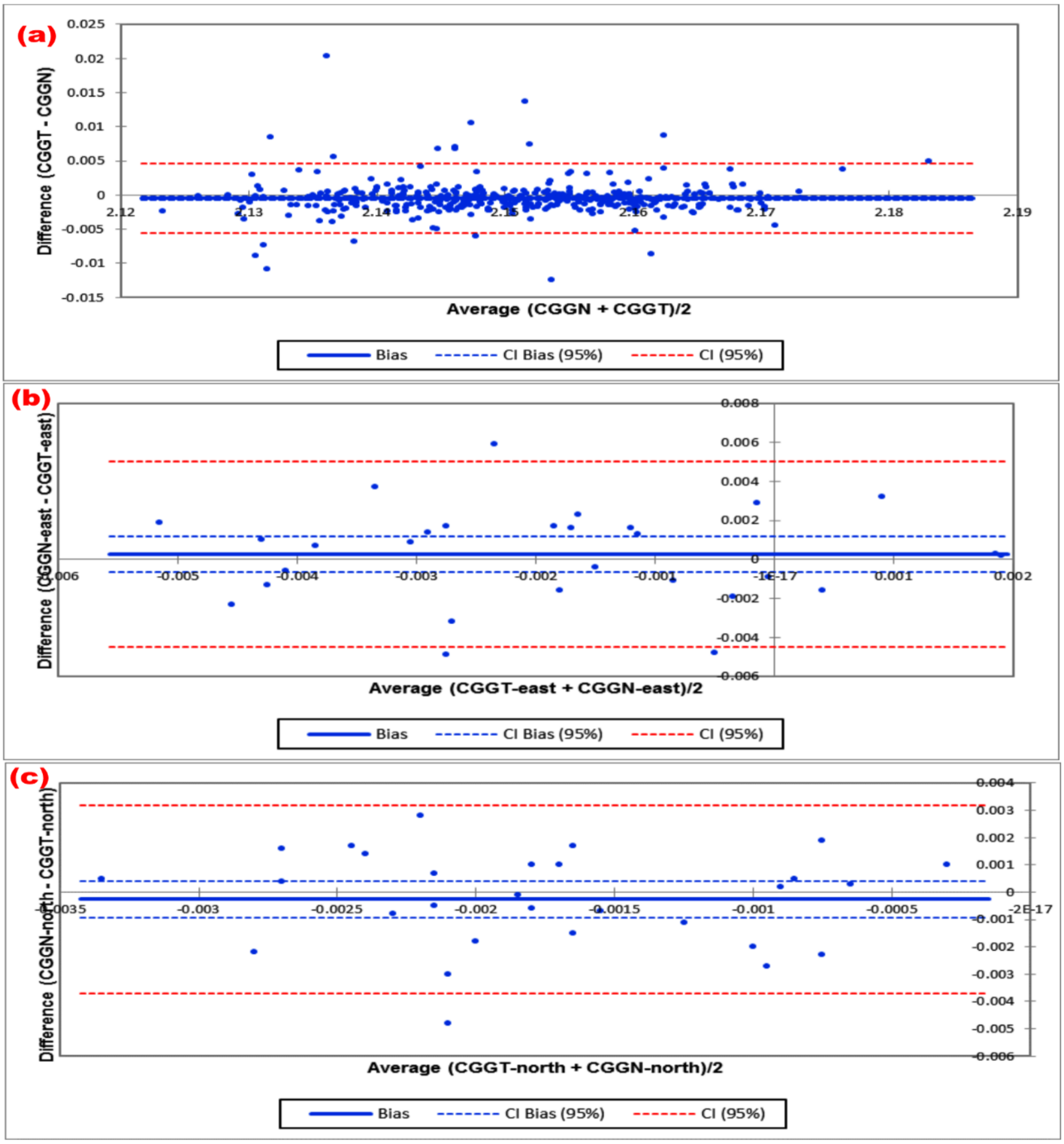

Figure 9: The Bland and Altman (difference) plot of estimated tropospheric parameters from the two receivers: a) is the ZTD in metres b) is the tropospheric gradient (east component) in metres and c) is the tropospheric gradient (north component) in metres

3.3 Receiver bias and TEC

From the box plot of the differences (Figure 10), the Bland and Altman estimate of bias is -54.4, and 0.541 for the receiver bias and TEC respectively. The confidence interval of the bias is between -55.235 and -53.565, with a standard error of 0.426; the receiver bias for CGGN was positive all through and out of the confidence level of the bias. In addition, from the time series plot (Figure 11), the maximum and minimum receiver bias stood at 14.600 and 1.100 for CGGT, and 39.000 and 53.000 for CGGN. The difference plot displays the difference between the estimated receiver bias from CGGN and CGGT against their average value, as shown in figure 11b. The estimated p-value from the Student t-test is < 0.000. Thus, the computed p-value is less than the significance level alpha = 0.05. The null hypothesis H_0 is rejected and the risk of rejecting the null hypothesis H_0 while it is true is lower than 0.01%. Scatter plot of estimated TEC from the dual receivers is shown in figure 12.

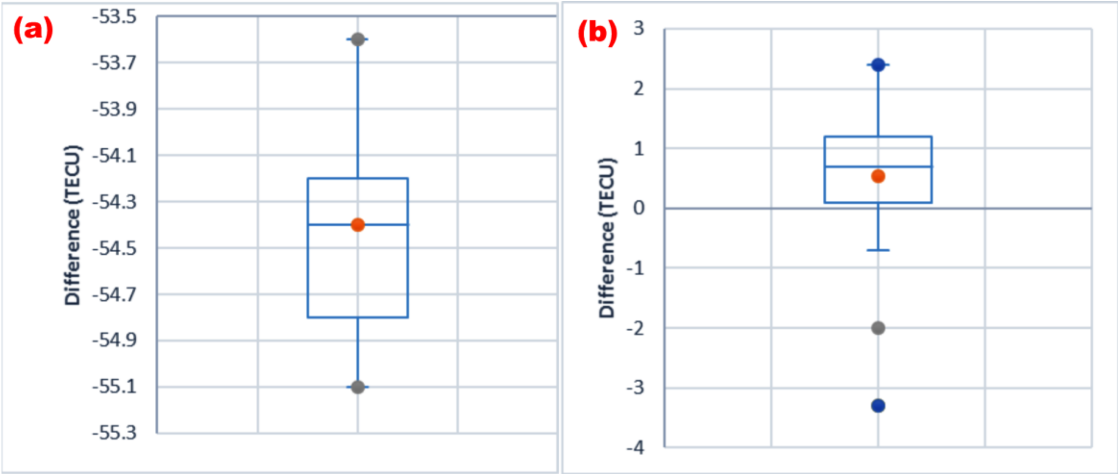

Figure 10: Box plot of differences in receiver bias and TEC estimations from the CGGN and CGGT

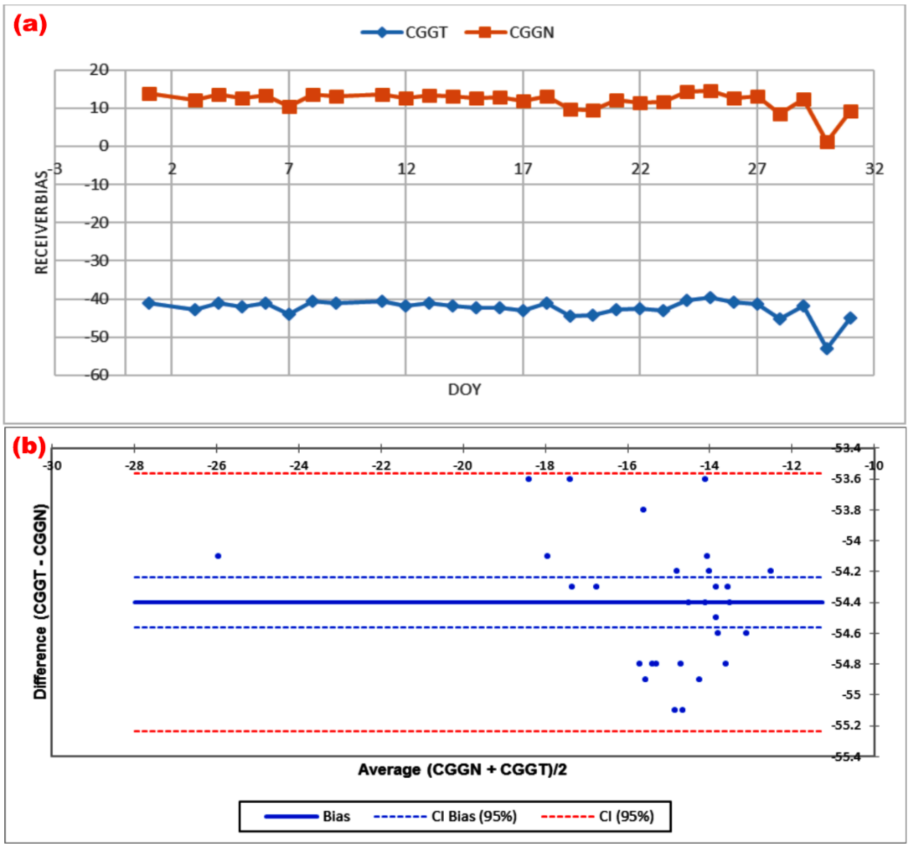

Figure 11: Receiver code bias estimated from the two receivers: a) Time series plot of estimated biases from the dual receivers b) Bland and Altman (difference) plot of estimated biases from the dual receivers

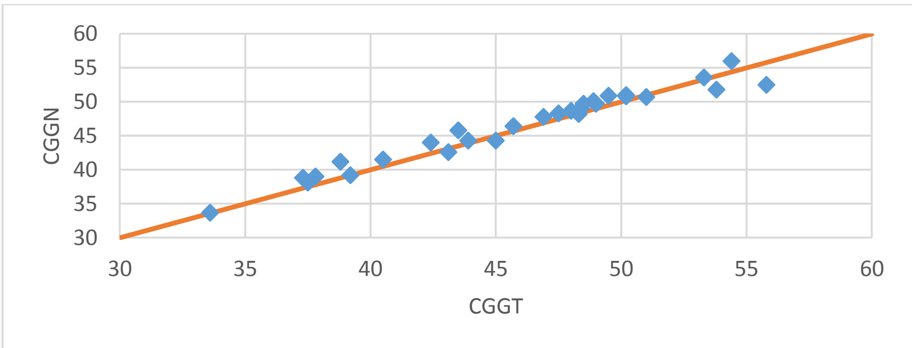

Figure 12: Scatter plot of estimated TEC from the dual receivers

The difference plot for the estimated TEC from CGGT and CGGN is shown in figure 13. The t-test result shows that if the computed p-value is lower than the significance level alpha = 0.05, one should reject the null hypothesis H_0, and accept the alternative hypothesis H_1. The risk of rejecting the null hypothesis H_0 while it is true is lower than 1.82%.

4.0 Concluding remarks

In this paper, a performance comparison test was carried out between two geodetic grade GNSS receivers at the CGG, Nigeria. The observatory at CGG remains the only geodetic observatory in Nigeria. The fact that CGG hosts an IGS site in Nigeria and that it is a proposed site for the global geodetic core network for collocation of GNSS and other space techniques underpinned this study. The results of the various comparison tests from this study are affirmative of the fact that the choice of GNSS receiver could significantly influence parameters estimated from data logged by them, as summarised in Table 4. Thus, we recommend further study of the performance of geodetic grade receivers over a longer period to study the possible effects of GNSS receiver clock stability adequately and it consequential effects on parameters estimated from them. The results of our study are preliminary in the sense that more complex statistical tests and a longer period are required to further validate how the differences observed in estimated parameters from receivers can influence scientific applications.

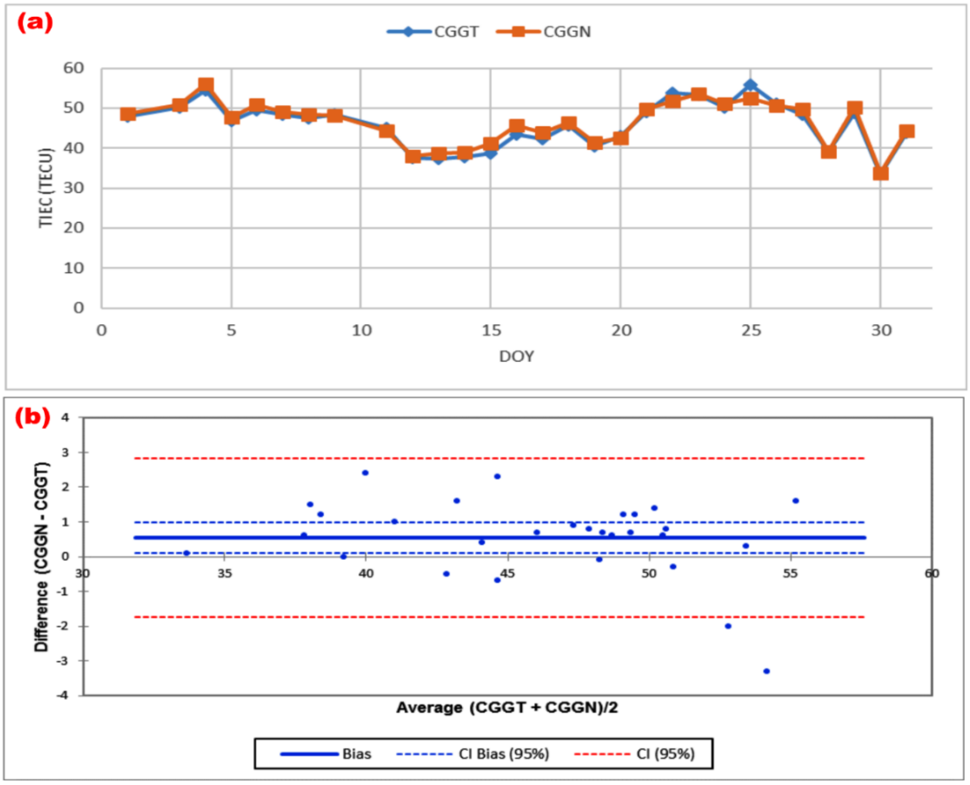

Figure 13: TEC estimated from the duo receiver: a) Time series plot of estimated TEC from the dual receivers b) Bland and Altman (difference) plot of estimated TEC from the dual receivers

Table 4: Summary of hypothesis test of estimated parameters

Estimate Parameters	**Hypothesis Test**	**Risk**
UTM Coordinate (Easting)	H_0 is not rejected	6.98%
UTM Coordinate (Northing)	H_0 is not rejected	16.51%
UTM Coordinate (Height)	H_0 is rejected and H_1 hypothesis accepted	0.59%
Tropospheric Zenith Delay	H_0 is rejected and H_1 hypothesis accepted	0.03%
Tropospheric Gradient (North Component)	H_0 is not rejected	43.97%
Tropospheric Gradient (East Component)	H_0 is not rejected	56.24%
Receiver Code Bias	H_0 is rejected and H_1 hypothesis accepted	0.01%
Total Electron Content	H_0 is rejected and H_1 hypothesis accepted	1.82%

Acknowledgement
The authors wish to express their profound gratitude to the numerous reviewers for their productive observations that helped to improve the manuscript. The authors thank CODE for making the DCBs files used in this study publicly available. We wish to thank the office of the Surveyor General of the Federal Republic of Nigeria and CDDIS for the GNSS data. Finally, thanks also go to Gopi Seemata for providing the GPS TEC analysis software and Prof Lambert Wanninger for the Wasoft software license.

References

Chuang, Y.C. and I. J. Gupta (2013). Antenna Induced Biases in GNSS Receiver Measurements. Proceedings of the International Technical Meeting of the Institute of Navigation. San Diego, CA, USA. (28–30): 164–171.

Cuntz, M., A. Konovaltsev, and M. Meurer (2016). Concepts, Development, and Validation of Multiantenna GNSS Receivers for Resilient Navigation. Proc. IEEE. (104):1288–1301. doi: 10.1109/JPROC.2016.2525764.

Dodo, J.D., T.A Yakubu, E.S. Usifoh, and A.M. Bojude (2011). ITRF 2008 Realization of the Nigerian Geocentric Datum (GDN2012): Preliminary Results. Journal of Emerging Trends in Engineering and Applied Sciences (JETEAS). 2(6):978-986.

Dow, J. M., R. E. Neilan, and C. Rizos (2009). The International GNSS Service in a Changing Landscape of Global Navigation Satellite Systems. *J Geod*, 83:191-198.

Gupta, I.J., I.M. Weiss, and A.W. Morrison (2016). Desired Features of Adaptive Antenna Arrays for GNSS Receivers. Proceedings of IEEE. (104):1195–1206. doi: 10.1109/JPROC.2016.2524416.

Isioye, O. A., L. Combrinck, and O. J. Botai (2017). Evaluation of Spatial and Temporal Characteristics of GNSS-derived ZTD Estimates in Nigeria. Theoretical and Applied Climatology, A publication of Springer-Verlag Wien, 1-18.

Isioye, O. A., L. Combrinck, and O. J. Botai (2017). Retrieval and Analysis of Precipitable Water Vapour Based on GNSS, AIRS, and Reanalysis Models over Nigeria. International Journal of Remote Sensing, 38(20): 5710-5735.

Jatau, B., M., Rui, A. Adeyemi, and G. Nuno (2010). NIGNET: The New Permanent GNSS Network of Nigeria. FIG Congress 2010: Facing the Challenges – Building the Capacity, Sydney: Australia. http://fig.net/pub/fig2010/papers/fs02h%5Cfs02h_jatau_fernandes_et_al_4549.pdf.

Kouba, J. (2009). A Guide to Using International GNSS Service (IGS) Products. Retrieved online from: http://igs.org/igscb/resource/pubs/UsingIGSProductsVer21.pdf

Moses, M., J. D., Dodo, and L. M. Ojigi (2017). Spatio-temporal and Solar Activity Variation of Ionospheric Total Electron Content over the Nigerian GNSS CORS. Conference of the Nigerian Association of Geodesy (NAG), Rivers State University, Port Harcourt, Rivers State, Nigeria, from 24th-27th October, 2017.

Naibbi, A. I. and S. S. Ibrahim (2014). An Assessment of the existing Continuously Operating Reference Stations (CORS) in Nigeria: An Exploration using Geographical Information System (GIS). American Journal of Geographic Information Systems, 3(4):147–157.

Odolinski, R. and P. Teunissen (2016). Single-frequency, Dual-GNSS versus Dual-frequency, Single-GNSS: a Low-cost and High-grade Receivers GPS-BDS RTK Analysis. Journal of Geodesy. 90(11): 1255-1278.

Schwieger, V. (2007). High-Sensitivity GPS – The Low Cost Future of GNSS. FIG Working Week, Hong Kong, 13-17 May, 2007. pp. 1-16.

Sousa, F. and F. Nunes (2014). Performance Comparison of a VDFLL versus VDLL and Scalar GNSS Receiver Architectures in Harsh Scenarios, ESA Workshop on Satellite Navigation User Equipment Technologies (NAVITEC), Noordwijk, Netherlands, Vol. 1, pp. 1 - 8

Takasu, T. and A. Yasuda (2008). Evaluation of RTK-GPS Performance with Low-Cost Single-Frequency GPS Receivers. Proceedings of International Symposium on GPS/GNSS, Tokyo. pp. 852-861.

Vagle, N., A., Broumandan, and G. Lachapelle (2016). Analysis of Multi-Antenna GNSS Receiver Performance under Jamming Attacks. Sensors (Basel, Switzerland). 16(11): 1937.